Stem Cell Reports
Article

ISSCR

OPEN ACCESS

Efficient Induction of Syncytiotrophoblast Layer II Cells from Trophoblast Stem Cells by Canonical Wnt Signaling Activation

Dongmei Zhu,[1,2,3,*] Xia Gong,[1,3] Liyun Miao,[1] Junshun Fang,[1] and Jian Zhang[1,2,*]
[1]State Key Laboratory of Molecular Developmental Biology, Institute of Genetics and Developmental Biology, Chinese Academy of Sciences, Beijing 100101, China
[2]State Key Laboratory for Conservation and Utilization of Bio-Resources, School of Life Sciences, Center for Life Sciences, Yunnan University, Kunming 650091, China
[3]Co-first author
*Correspondence: dmzhu@genetics.ac.cn (D.Z.), jianzhang84@genetics.ac.cn (J.Z.)
https://doi.org/10.1016/j.stemcr.2017.10.014

SUMMARY

The syncytiotrophoblast layer is the most critical and prominent tissue in placenta. SynT cells are differentiated from trophoblast stem cells (TSCs) during early embryogenesis. Mouse TSCs can spontaneously differentiate into cells of mixed lineages *in vitro* upon withdrawal of stemness-maintaining factors. However, differentiation into defined placental cell lineages remains challenging. We report here that canonical Wnt signaling activation robustly induces expression of SynT-II lineage-specific genes *Gcm1* and *SynB* and suppresses markers of other placental lineages. In contrast to mouse TSCs, the induced SynT-II cells are migratory. More importantly, the migration depends on hepatocyte growth factor (HGF) and the c-MET signaling axis. Furthermore, HGF-expressing cells lie adjacent to SynT-II cells in developing murine placenta, suggesting that HGF/c-MET signaling plays a critical role in SynT-II cell morphogenesis during the labyrinth branching process. The availability of SynT-II cells *in vitro* will facilitate molecular understanding of labyrinth layer development.

INTRODUCTION

The placenta is a temporary but essential organ for mammalian embryonic development. Through the placenta, mother and fetus exchange nutrients, oxygen, and wastes (Maltepe et al., 2010; Rossant and Cross, 2001). Placenta protects the fetus from maternal immune attacks (Moffett and Loke, 2006). In addition, the placenta also serves as a niche in which hematopoietic stem cells rise during mouse and human embryonic development (Mikkola et al., 2005; Robin et al., 2009). Aberrant placental development in humans can result in pathological defects, such as preeclampsia, intrauterine growth restriction (IUGR), and even fetal death (Unek et al., 2017).

Mature mouse placenta contains three layers: the outermost trophoblast giant cell (TGC) layer, middle junctional zone spongiotrophoblast (SpT) layer, and the innermost labyrinth layer. The labyrinth layer plays critical roles in material exchanging between the mother and her fetus. The mouse labyrinth layer contains two adjacent trophoblast cells, syncytiotrophoblast layer I (SynT-I) and layer II (SynT-II), which separate and regulate material exchanges between maternal blood sinuses and fetal blood vessels (Simmons et al., 2008a). In the mouse, all the trophoblastic cells are developed from trophectoderm at E3.5 blastocyst and later extra-embryonic ectoderm at embryonic day 6.5 (E6.5) stage. Multipotent trophoblast stem cells (TSCs) can also be derived from embryos at these two stages and maintained in culture with fibroblast growth factor 4 (FGF4) and mouse embryonic fibroblast cell-conditioned medium (MEF-CM) (Asanoma et al., 2011; Hayakawa et al., 2015; Quinn et al., 2006; Tanaka et al., 1998). Upon withdrawal of the maintenance factors, TSCs spontaneously differentiate into mixed lineages of placental trophoblastic derivatives *in vitro*. TSCs can preferentially differentiate into TGC by addition of retinoic acid and diethylstilbestrol in monolayer 2D culture, or 3D trophosphere culture (Rai and Cross, 2015; Tremblay et al., 2001; Yan et al., 2001), but the other trophoblast lineages, such as SynT layers, have not been fully examined.

In mature murine placenta, the labyrinth zone takes the majority of the volume of placenta to support fetus growth. Mouse mutants with an underdeveloped labyrinth (small labyrinth) die at mid-gestation stage (Watson and Cross, 2005), suggesting fully branched SynT cells are critical for normal labyrinth formation. However, labyrinth morphogenesis remains an unanswered but important question in the field.

At E8.5, the extra-embryonic mesoderm-derived allantois reaches and attaches to the extra-embryonic ectoderm chorion trophoblast cells (chorioallantoic attachment), forming a combined and flattened tissue, followed by SynT-II cell specification and branching. Wnt signaling is essential for these processes. *Wnt7b* null mice die at mid-gestation stages due to impaired chorioallantoic attachment (Parr et al., 2001). Mutant mice with deletion of several components of Wnt signaling, such as *R-Spondin3* (Aoki et al., 2007), *Bcl9* (Matsuura et al., 2011), and *Frizzled 5* (*Fzd5*) (Ishikawa et al., 2001), show severe defects in SynT-II specification and branching initiation. *Wnt2* deletion causes perinatal embryonic death with defect of labyrinth development, although at a slightly later stage

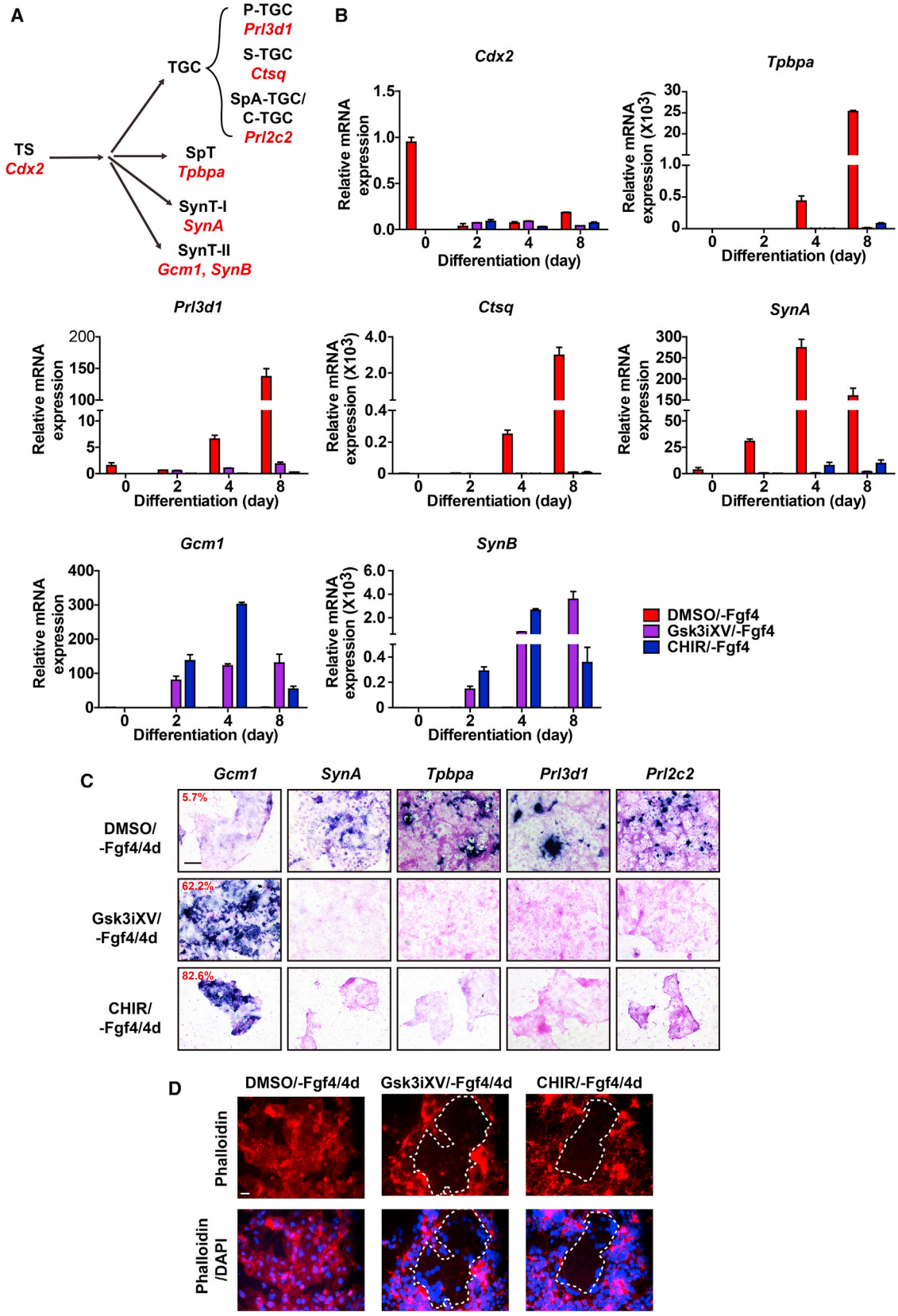

(legend on next page)

(Monkley et al., 1996). The chorioallantoic attachment is associated with activation of canonical Wnt signaling through *Fzd5*, at least partly by Wnt2 ligand. The activation of Wnt signaling is necessary for upregulation of transcription factor glial cell missing 1(*Gcm1*) and SynT-II cell specification (Lu et al., 2013; Matsuura et al., 2011). Since E9.5, the *Gcm1*-positive cells label the tip cells of the initial branching labyrinth (Simmons et al., 2008a). However, whether *Gcm1*-positive cells actively lead the remaining cells or they are passively pushed to the front has not been resolved.

Cell migration plays essential roles during organogenesis. TGCs and glycogen trophoblast cells are invasive during placenta development. TGCs mediate the invasion of the implanted embryos into the maternal decidua (Simmons et al., 2007). Both TGC and glycogen cells are implied for remodeling the endothelium-lined artery to trophoblast-lined sinus (Adamson et al., 2002). Whether cells of other trophoblastic lineages have migration capability is unknown.

Multiple signaling pathways are involved in initiating and maintaining cell migrations. The hepatocyte growth factor (HGF)/c-MET pathway mediates signal exchange between mesenchyme and epithelia during morphogenesis in several tissues, including developing kidney, mammary gland, and lung (Imamura and Matsumoto, 2017; Nakamura et al., 2011). During mouse placenta development, deletion of either *Hgf* or *c-Met* genes causes embryonic death in utero due to an underdeveloped labyrinth (Uehara et al., 1995; Ueno et al., 2013). HGF/c-MET signaling has also been implicated in human trophoblastic cell invasion (Dokras et al., 2001; Nasu et al., 2000). Reduced expression of HGF is also correlated with human pregnancy pathologies, IUGR and pre-eclampsia (Chen, 2014; Somerset et al., 1998).

In this study, we show that activation of canonical Wnt signaling is sufficient to promote SynT-II cell differentiation from TSCs but suppresses differentiation of all other trophoblastic lineages. Moreover, we reveal that SynT-II cells are highly migratory and display collective migration behavior. We further show that the migration is dependent on HGF/c-MET signaling. The availability of SynT-II cells *in vitro* should help dissect how the interface between mother and fetus is established at molecular level.

RESULTS

Activation of Canonical Wnt Signaling Robustly Induces Mouse TS Cell Differentiation into Trophoblast SynT-II Cells

Terminally differentiated somatic cells from stem cells are useful for studying their functions *in vitro* and may also be used for cell-replacement therapy. For placental cell differentiation, cultured mouse TSCs can differentiate into mixed trophoblastic lineages upon withdrawal of FGF4 and MEF-CM (Figure 1A) (Tanaka et al., 1998). However, efficient differentiation of specific trophoblastic cell lineages has yet to be established *in vitro*. Previous *in vivo* studies indicated that Wnt signaling is required for trophoblast SynT-II cell differentiation and labyrinth development (Lu et al., 2013; Sonderegger et al., 2010). This requirement was confirmed by knocking down *β-catenin* expression, which impaired SynT-II cells differentiation (Figure S1A). Despite the requirement of Wnt for SynT-II differentiation, molecules sufficient to induce SynT-II are unknown. Wnt and other factors expressed in early placenta are clearly candidates.

First, we set to test whether Wnt activation alone is sufficient to induce SynT-II cell differentiation *in vitro*. To this end, we used specific GSK3β inhibitors Gsk3iXV and CHIR99021 (CHIR), which stabilize β-catenin protein (Figure S1B) to activate the canonical Wnt signaling in cultured TSCs. In the presence of stemness factors, activation of canonical Wnt signaling did not change either morphology of TSCs (data not shown) or expression of TSC stemness markers *Cdx2* and *Eomes* (Figure S1C). Next, we designed a different protocol by withdrawal of FGF4 and MEF-CM but addition of Gsk3iXV or CHIR. In either DMSO (control)- or Gsk3β inhibitor-treated cells, *Cdx2* expression

Figure 1. Activation of Canonical Wnt Signaling Is Sufficient for Trophoblastic SynT-II Cell Differentiation

(A) A dendrogram shows lineages derived from trophoblast stem cells and their respective markers (in red). TS, trophoblast stem cells; TGC, trophoblast giant cell; P-TGC, parietal TGC; S-TGC, sinusoidal TGC; SpA-TGC, spiral-associated TGC; C-TGC, canal TGC; SpT, spongiotrophoblast; SynT-I, syncytiotrophoblast layer I; SynT-II, syncytiotrophoblast layer II.

(B) Expression of different lineage markers measured by qRT-PCR under three differentiation protocols. DMSO, Gsk3iXV, and CHIR indicate TSCs treated with the respective molecules, meanwhile withdrawing stemness factors. qRT-PCR data were normalized to *Gapdh* and represented as mean ± SEM. Data were summarized from three independent experiments, and each experiment had two technical repeats.

(C) Expression of different lineage markers measured by RNA *in-situ* hybridization at the fourth day of differentiation treated with indicated DMSO, CHIR, or Gsk3iXV. Scale bar, 200 μm. Percentages of Gcm1-positive cells are shown.

(D) F-Actin in differentiated cells and nuclear staining at the fourth day of differentiation under DMSO, Gsk3iXV, or CHIR treatment. Dashed lines indicate syncytial cell boundaries. Phalloidin stains F-actin; DAPI counterstains cell nuclei. Scale bar, 50 μm.

See also Figures S1 and S2.

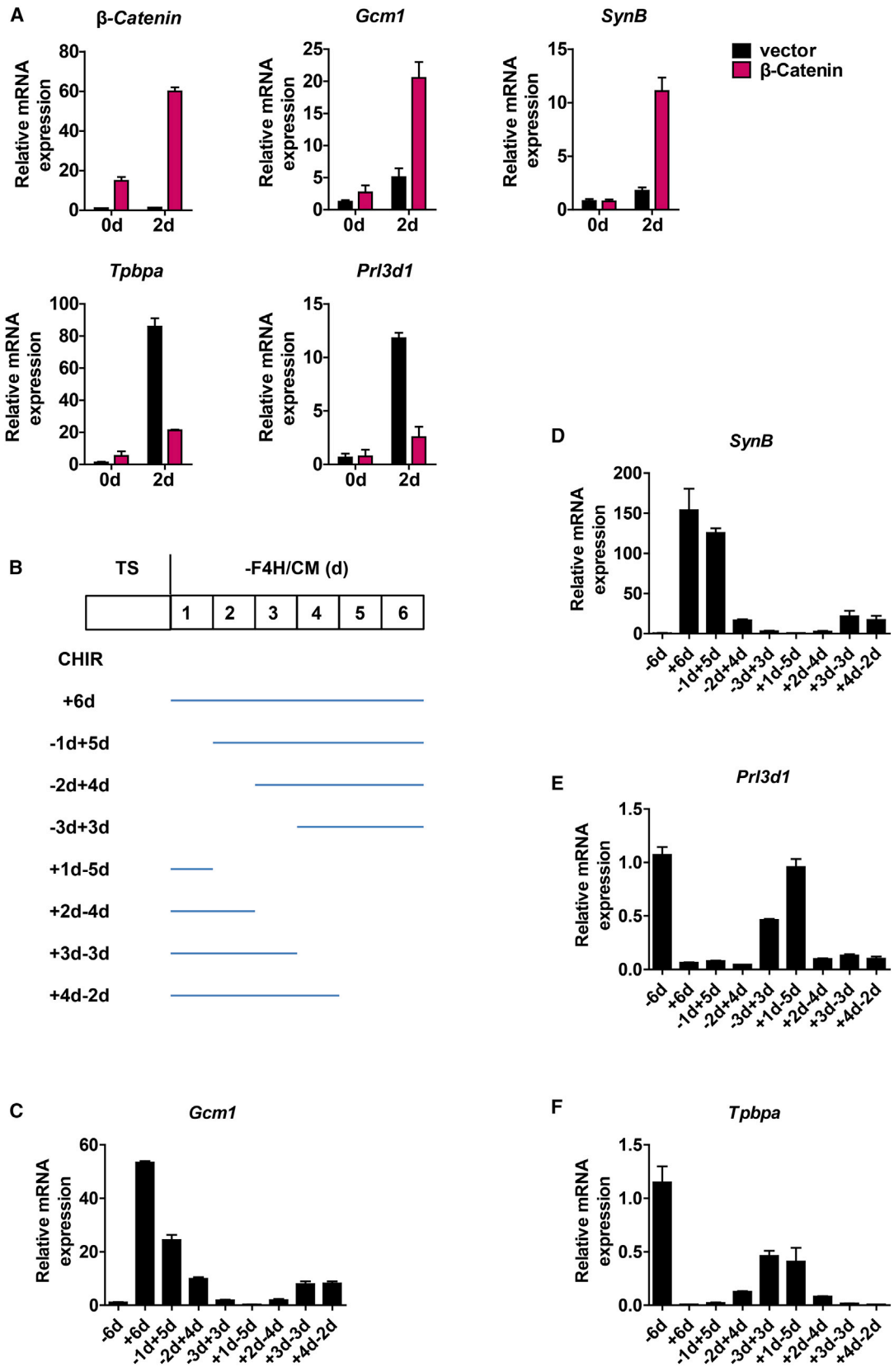

(legend on next page)

decreased drastically upon withdrawal of stemness-maintaining factors (Figure 1B). In the control cells, trophoblastic lineages markers were upregulated compared with TSCs 2 days after the procedure started. In contrast, in Gsk3iXV and CHIR-treated cells, *Tpbpa* (an SpT and glycogen trophoblast cell marker), *Prl3d1* (*PL-1*) (a parietal TGC marker), and *Cathepasin Q* (*Ctsq*) (a sinusoidal TGC marker) were barely detected, but *Gcm1* and *SynB* (SynT-II cell-specific markers), were drastically upregulated (Figure 1B). It should be noted that although labyrinth trophoblast SynT-I and SynT-II are spatially and functionally associated to each other, expression of *SynA* (a SynT- I marker) was largely unchanged, suggesting that SynT-I differentiation is controlled by a distinct mechanism (Figure 1B). RNA *in-situ* hybridization results also confirmed that robust SynT-II differentiation from TSCs after CHIR or Gsk3iXV treatment (Figure 1C). *Gcm1*-positive cells in CHIR (62.2%)- or Gsk3iXV (82.6%)-treated groups are much more than those in the DMSO control (5.7%) group. Lack of expression of *Prl3d1*, *Prl2c2*, and *Ctsq* suggests that differentiation of all four types of TGCs (parietal TGC, sinusoidal TGC, spiral-associated TGC, and canal TGC) were suppressed in Gsk3β inhibitor-treated cells (Figures 1B and 1C) (Simmons et al., 2008b). Suppression of TGC differentiation was further confirmed by the lack of polyploid nuclei, which is a feature of TGCs by endoreduplication (Simmons et al., 2007). DNA content can be used to estimate the percentage of cells with polyploid mononuclear cells. We used flow cytometry (fluorescence-activated cell sorting) to check DNA content on differentiated cells with or without the inhibitors. In undifferentiated TSCs (Di-0d), there was a low percentage (10.4%) of spontaneous differentiated cells, with DNA content larger than 4 N. For DMSO-treated cells, there were 21.1% and 36.4% polyploid cells at day 4 and day 6, respectively (Figure S2). In contrast, upon Wnt activation by the inhibitors, the percentages of polyploid cell population remained relatively low on differentiation day 4 (12.8%) and day 6 (15.1%), which were marginally higher than those in TSCs spontaneous differentiated (Figure S2), indicating TGC differentiation was inhibited.

Cell fusion typically occurs during normal development of trophoblast syncytia layer I and II (Huppertz and Gauster, 2011). Consistent with robust SynT-II cell marker expression upon Wnt activation, cell fusion was observed in densely seeded cells by filamentous actin and nuclei staining (Figure 1D). To confirm that canonical Wnt signaling drives SynT-II cell differentiation, we overexpressed the constitutive active form of human β-catenin (S37A) in TSCs, which resulted in SynT-II differentiation, as expected (Figure 2A).

Next, we examined timing of Wnt signaling required for the SynT-II differentiation. We added CHIR, a reversible Gsk3β inhibitor, to the culture system and washed it out at different time points (Figure 2B). Cells were harvested after a 6-day culture for gene expression analysis. The expression of *Gcm1* and *SynB* were reversely correlated to the expression of *Prl3d1* and *Tpbpa* (Figures 2C–2F). Although addition of CHIR in the entire procedure induces the highest level of *Gcm1* and *SynB*, supplement of the inhibitor from day 2 still induced high expression of the SynT-II markers. In contrast, addition of CHIR from day 4 abolished the marker expression, suggesting the second to the third day is the key window for SynT-II cell specification in the protocol (Figures 2C and 2D). Suppression of TGCs and SpT cell lineages also supported the window is critical for SynT-II differentiation (Figures 2E and 2F). Collectively, we conclude that canonical Wnt signaling activation is sufficient for TSC differentiation into SynT-II cells, and for suppressing other trophoblastic lineages.

SynT-II Cells Actively Migrate in Culture

Upon withdrawal of FGF4 and MEF-CM, TSCs differentiate into mixed trophoblastic cell types, in which the TGCs are the dominant cell type. Previous *in vitro* studies confirmed that TGCs have migration and invasion capability (Hemberger et al., 2004). Although SynT-II cells are involved in the labyrinth branching morphogenesis, whether they have migratory capacity remains unknown, partly due to lack of isolated SynT-II cells. To address this question, we tracked induced SynT-II cells under a spinning disc confocal microscope for 6 hr. Time-lapse images were taken every 90 s. SynT-II cells migrated with active lamellipodia extension and retraction, while TSCs remain stationary (Figure 3A). Similarly, in a wound-healing assay for cultured cells, SynT-II cells migrated and closed scratched gaps within 48 hr (Figure 3B). We further tested SynT-II invasive capability in a transwell assay. Equal numbers of

Figure 2. Overexpression of *β-Catenin* Is Sufficient for SynT-II Cell Differentiation

(A) Expression of *β-catenin* and differentiation markers measured by qRT-PCR in TSCs transfected with vector or *β-catenin* (S37A, constitutive active form) plasmids. Data were summarized from three independent experiments, and each experiment had two technical repeats.

(B) Schemes of CHIR treatment at defined time points during the differentiation protocol. Solid lines indicate the presence of CHIR.

(C–F) qRT-PCR analyses of mRNA expression levels of *Gcm1* (C), *SynB* (D), *Prl3d1* (E), and *Tpbpa* (F) at the sixth day of differentiation indicated in (B). qRT-PCR data were summarized from three technical repeats, normalized to *Gapdh* expression, and represented as mean ± SEM.

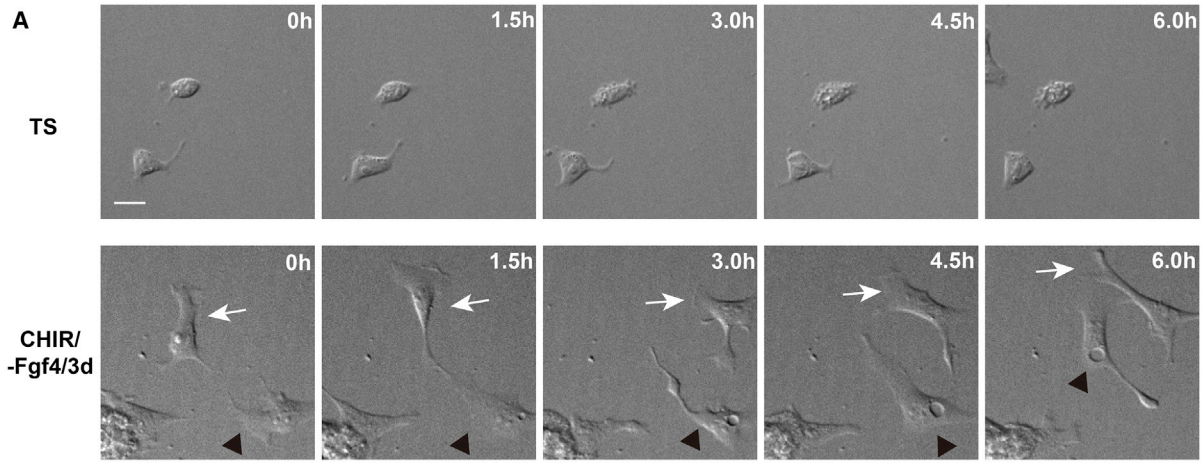

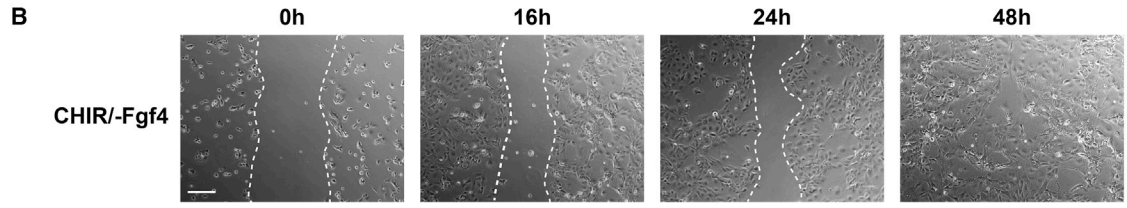

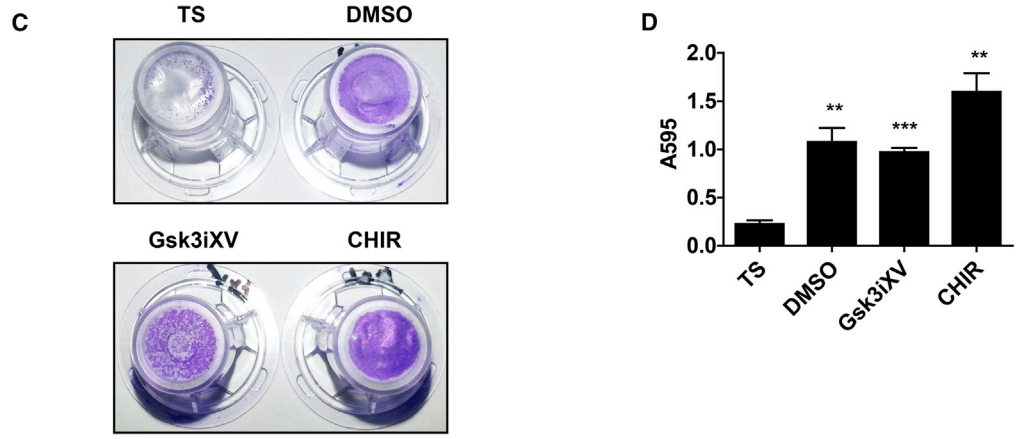

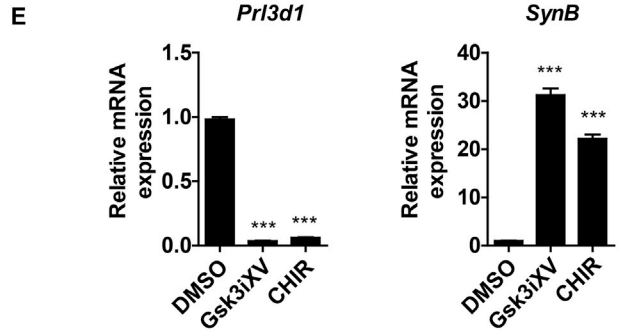

(legend on next page)

differentiated cells and undifferentiated TSCs were seeded into Matrigel-coated transwells. Forty-eight hours later, after removing the cells in the upper chamber, cells on the bottom membrane were stained with crystal violet. Consistent with the time-lapse migration result, undifferentiated TSCs showed little invasion capacity (Figure 3C). DMSO-treated differentiated cells consisting of TGCs, which are highly migratory, actively invaded the transwell membrane. SynT-II cells induced by CHIR or Gsk3iXV show comparable invasion with DMSO-treated cells (Figure 3C). It should be noted that the SynT-II induction protocol does not generate TGC differentiation (Figures 1B, 1C, and S2). Quantitative analysis of crystal violet-positive cells on the bottom side confirmed that the SynT-II cells were significantly more invasive compared with TSCs (Figure 3D). qRT-PCR analyses showed that the invaded cells (collected from the bottom side of the transwell) in the DMSO group highly expressed TGC marker *Prl3d1*, but not of *SynB*. In contrast, SynT-II cells showed high *SynB* expression, but low *Prl3d1* (Figure 3E). This further confirms that the invading cells in the DMSO group were mainly TGCs, while the inhibitors-treated cells were SynT-II cells. Furthermore, SynT-II cells had more uniform and flat morphology than DMSO-treated cells (Figure S3). In summary, in addition to TGCs and glycogen cells, we identify SynT-II cells as another type of migratory cells in placenta.

Epithelial Mesenchymal Transition Is Not Involved in SynT-II Cell Migration

Epithelial mesenchymal transition (EMT) is required for certain cells to obtain migratory capability. Previous studies showed that EMT occurs during TSC differentiation (Abell et al., 2009). We examined whether EMT played a role for SynT-II cells to acquire migration capability. First, we checked DMSO-treated cells and found that, consistent with previous reports, the EMT hallmark *E-cadherin* was downregulated (Yang and Weinberg, 2008), while the EMT inducer *Snail1* was significantly upregulated (Figure 4A) (Abell et al., 2009, 2011). In contrast, in SynT-II cells *Snail1* was largely unchanged, but another EMT inducer, *Zeb2* (*SIP1*), was upregulated (Figure 4B) (Comijn et al., 2001). In addition, *E-cadherin* expression was not repressed (Figure 4B). Prolonged differentiation also gave similar results (Figure 4C). Furthermore, immunofluorescent staining results indicated that ZEB2 protein localizes at the cell-cell boundary and in nuclei of cells treated with DMSO or CHIR (Figure S4A). Similar to the qRT-PCR results, ZEB2 protein expression was higher in SynT-II cells than control cells (Figure S4A). ZEB2 was reported to be a multi-zinc-finger protein that downregulates *E-cadherin* in the process of EMT (Comijn et al., 2001). However, the ZEB2 expression pattern suggests that it unlikely functions as a transcriptional repressor in trophoblast cells. In addition to *E-cadherin*, neither placenta cadherin (*P-cadherin, Cdh3*) nor tight junction marker (*Zo-1*) was downregulated in SynT-II cells (Figure 4C). Consistent with their invasive behavior, both DMSO control and SynT-II cells showed high expression level of cell matrix metalloproteinase *Mmp14* (TP-Mmp), which is required for the digestion of extracellular matrix (Figure 4C). We further examined E-cadherin expression in E9.5 mouse placenta, the labyrinth branching initiation stage, and confirmed that E-cadherin was not downregulated in the branching tip (Figure S4B). These results suggest that EMT does not occur at the beginning of labyrinth branching morphogenesis, and EMT is unlikely required for SynT-II cells to acquire migration capability.

In addition to individual cell migration, such as that of leukocytes, cells can also migrate in associated groups or collective migration. In both mouse and human placenta, SynT cells are fused to form multinucleated syncytin layer. As shown in Figure 4D, migratory SynT-II cells show strong cell-cell adherent junction. For collective cell movement, high phosphor-Ser19-myosin light chain (pS-MLC), around the outer cell clusters, and low inside cell clusters is required to generate actomyosin contractility (Hidalgo-Carcedo et al., 2011). SynT-II cells likely migrate collectively *in vitro*. First, immunofluorescent staining results showed a stronger signal of pS-MLC around the edge of SynT-II cell clusters, but not in DMSO-differentiated cells,

Figure 3. SynT-II Cells Have Migration Capability

(A) Time-lapse images of undifferentiated TSCs and CHIR-induced SynT-II cells. White arrows and black arrowheads indicate two different migration cells, respectively. Scale bar, 20 μm.

(B) Wound-healing assay results of SynT-II cells at 0, 16, 24, and 48 hr after scratch of confluent cells. Dashed lines represent edges of the cell population. Scale bar, 20 μm.

(C) Invasion analysis of undifferentiated TSCs and differentiated cells after administration of DMSO, Gsk3iXV, or CHIR for 2 days. Representative pictures of crystal violet staining show the invaded cells at the bottom membranes.

(D) Quantification of the invaded cells indicated in (C). Data are represented as mean ± SEM. Error bars were calculated from three independent experiments.

(E) RNA expression of *Prl3d1* and *SynB* of invaded cells from indicated differentiation protocols. qRT-PCR data were summarized from three independent experiments, normalized to *Gapdh* expression, and represented as mean ± SEM.

**p < 0.01; ***p < 0.001. See also Figure S3.

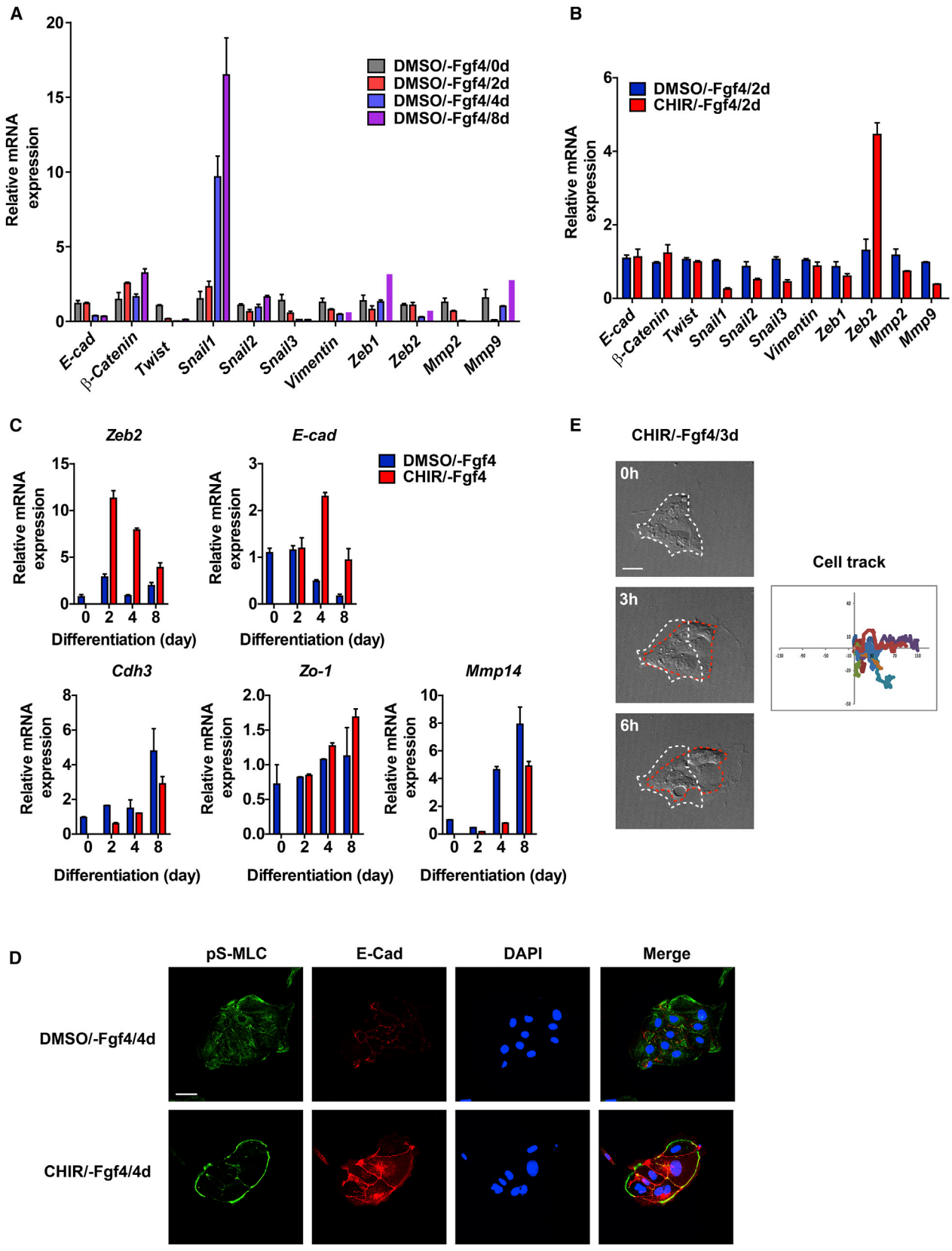

(legend on next page)

whose migration of mainly TGCs (Figure 3E) depends on EMT (Abell et al., 2009) (Figure 4D). Second, time-lapse imaging and individual cell tracking indicated that cells within a cluster migrated as a group (Figure 4E; Movie S1). Together with previous observations, our results strongly suggest that SynT-II cells migrate collectively.

HGF/c-MET Signaling Induces SynT-II Cell Migration

In mouse placenta, syncytiotrophoblast cells develop and integrate into highly branched structures in the mature labyrinth zone. Development of full labyrinth structure is tightly controlled. What signaling pathway regulates SynT-II cell migration is unknown. Mouse mutants of MAPK-ERK signaling pathway components showed various degrees of underdeveloped labyrinth, such as: *Mek1*, *Erk2*, *Grb2*, *Gab1*, *Sos1*, and *Raf1*. Similar phenotypes were also observed for mutants of *Fgfr2*, *Hgf*, *c-Met*, and *Egfr*, which are ligands or receptors upstream of MAPK-ERK signaling (Hatano et al., 2003; Watson and Cross, 2005), suggesting that the pathway may be required for SynT-II cells migration.

To examine possible roles of MAPK-ERK signaling in SynT-II cell migration, we used MEK1/2 inhibitors in the transwell invasion assay. As shown above, SynT-II cells robustly invaded the Matrigel, while MEK1/2 inhibitors PD0325901, PD98059, or CI-1040 reduced SynT-II cells invasion (Figure 5A). Rho signaling has a central role for cell polarity and motility through regulation of the cell skeleton (Ridley, 2015). Since SynT-II cells migrated with active lamellipodia extension and retraction (Figure 4E; Movie S1), ROCK2 inhibitor Y27632, as expected, also impaired SynT-II cell migration (Figure 5A). A number of ligands could activate intracellular MAPK signaling through binding to their respective receptors. We set out to look for ligand-receptor pair functions upstream of the MAPK-ERK pathway in SynT-II cells. FGF signaling is one of the candidates. qRT-PCR examination of all the paracrine FGF ligands and receptors indicated that high expression level of *Fgf2* (*bFgf*), Fgfr1, and *Fgfr2* in mouse E10.5 placenta (Figure S5A). However, neither FGF2 protein nor pan-FGF receptor inhibitor affect SynT-II cell invasion in the transwell assay (Figure 5B). Furthermore, none of the examined inhibitors of epidermal growth factor receptor, platelet-derived growth factor receptor, vascular endothelial growth factor, and CXCR4 impaired SynT-II cells invasion, either (Figures 5B and S5B).

HGF and its receptor c-MET were reported to be essential for mouse and human placenta development (Dokras et al., 2001; Uehara et al., 1995). c-MET, a receptor tyrosine kinase is one of the upstream activators for MAPK/ERK signaling (O'Brien et al., 2004). c-MET inhibitors were used in the SynT-II cell invasion assay and all significantly reduced the SynT-II cell invasion (Figure 5C). Inhibition of the downstream factors of the c-Met pathway, bRAF and MEK1/2, also reduced the cell invasion (Figure 5C). This result suggests that HGF/c-MET, through downstream RAF and MEK signaling, regulates SynT-II cell motility. We also observed that *c-Met* mRNA expression was increased in SynT-II cells, but not in CHIR-treated TSCs in the presence of stemness factors (Figure 5D). Western blot data confirmed that c-MET increased in SynT-II cells as well. Meanwhile, the activated form of MEK1/2, phosphor-MEK1/2, increased dramatically (Figure 5E), indicating MEK signaling was activated in SynT-II cells. Immunohistochemistry data showed that c-MET specifically expressed in the mouse placenta labyrinth zone (Figure 5F). Co-localization of c-MET with monocarboxylate transporter 4, which specifically expresses on SynT-II layer (Nagai et al., 2010), confirmed that c-MET expresses on SynT-II cells *in vivo* (Figure 5F).

Next, we tested the effect of HGF on SynT-II cell migration. To visualize the source of HGF in placenta, *Hgf in-situ* hybridization was performed. From E9.5, the beginning of labyrinth branching, to mature placenta at E14.5, *Hgf* localizes at the basal allantois mesenchyme adjacent to c-MET-positive SynT-II cells (Figures 6A and 6B). In the

Figure 4. Epithelial Mesenchymal Transition Is Not Involved in SynT-II Cell Migration

(A) RNA expression of EMT-related markers were measured by qRT-PCR during trophoblastic cell differentiation by withdrawal of FGF4 and MEF-CM.

(B) RNA expression of indicated EMT-related genes was measured by qRT-PCR at differentiation day 2. Cells were treated with DMSO or CHIR.

(C) RNA expression of *Zeb2*, *Cdh1*, *Cdh3*, *Zo-1*, and *Mmp-14* was measured by qRT-PCR. Cells were treated with DMSO or CHIR at indicated time.

(D) Double immunofluorescent staining of pS-MLC and E-cadherin of cells after 4 days of DMSO or CHIR treatment. DAPI labels cell nuclei.

(E) Time-lapse images of a SynT-II cell cluster. White dashed line circles the original position of the cluster, and red dashed lines labels positions at indicated recording time. Positions of individual cells (represented by different colors) in the cluster at different time points were tracked and recorded in the right plot with ImageJ software.

qRT-PCR data in (A), (B), and (C) were summarized from three independent experiments, normalized to *Gapdh* expression, and represented as mean ± SEM. Scale bars, 50 μm in (D and E).

See also Figure S4.

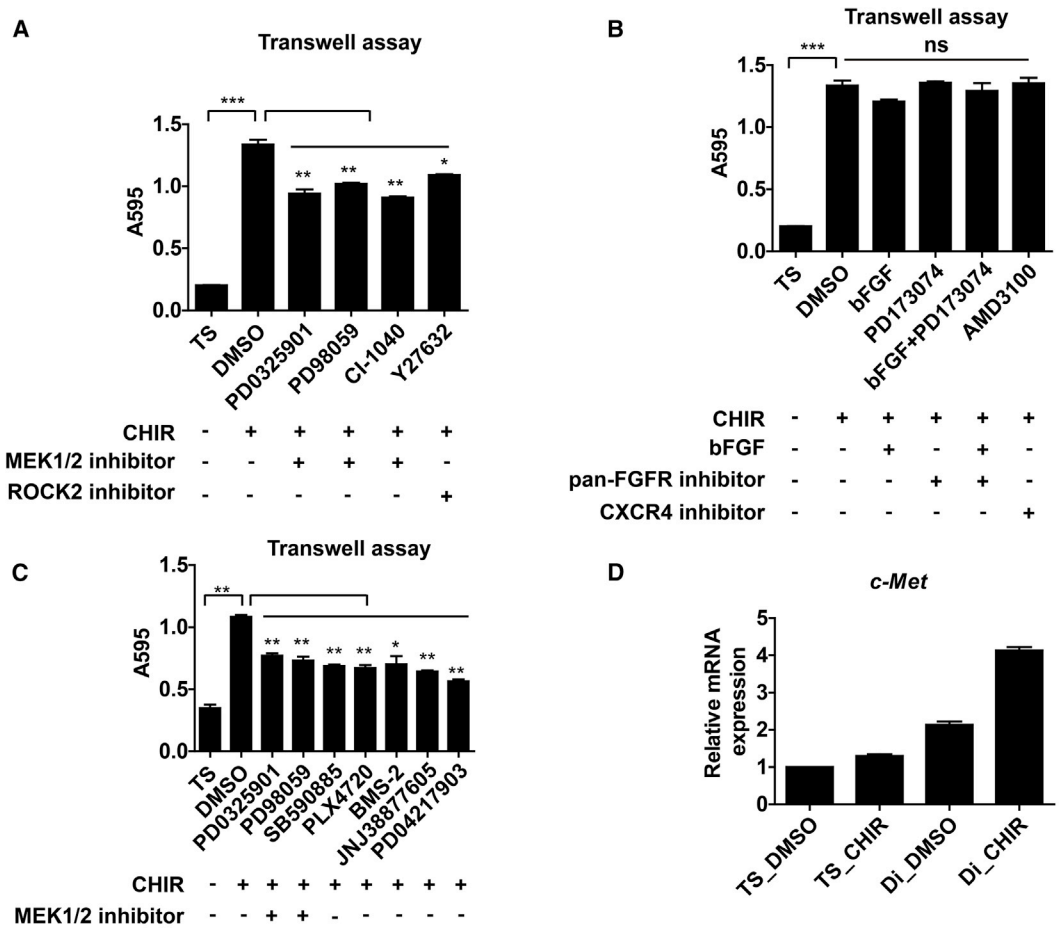

(legend on next page)

transwell assay, recombinant HGF protein dose-dependently increased invasiveness of SynT-II cells (Figure 6C). Addition either c-MET inhibitor or downstream signaling MEK1/2 inhibitor reversed the phenotype (Figure 6D, left panel). HGF/c-MET signaling was reported to be required for the proliferation of labyrinth trophoblast progenitor cells, which can differentiate into all labyrinth trophoblastic cell subtypes (Ueno et al., 2013). We set to test whether HGF affects SynT-II cell proliferation. Although HGF significantly increased SynT-II cell migration, it did not change their proliferation rate (Figure 6D, right panel). Addition of G1/S inhibitor, thymidine, which is commonly used for cell-cycle synchronization and cell proliferation blocker (Ma and Poon, 2017), confirmed that HGF promoted SynT-II cell migration irrespective of cell proliferation (Figure S5C). We also recorded the migration of SynT-II cells in the presence of CHIR with or without HGF and/or c-MET inhibitor using spinning disc confocal microscopy. The relative velocity of the migrating cells was calculated by tracking individual nuclei. The results indicated that HGF significantly increased SynT-II cell moving, while c-MET inhibitor reversed the phenomenon (Figure 6E). We conclude that HGF/c-MET ligand-receptor axis, acting through downstream MAPK/ERK signaling, regulates SynT-II cell migration.

DISCUSSION

Dissection of maternal-fetal interface development has been one of the major goals in placenta biology. In this study, we found that activation of canonical Wnt signaling is sufficient for induction of trophoblast SynT-II cells from TSCs in culture. We further showed that SynT-II cells have collective migration and invasion capability. Finally, the migration is regulated by HGF/c-MET and via intracellular MAPK-ERK signaling. The availability of SynT-II cells provides a useful tool to study development of the branching labyrinth.

Wnt signaling pathway is critical for placenta development, including SynT-II cell differentiation. Previous studies indicated that a low level of *Gcm1* expression could be detected as early as E7.5 (1 day before chorioallantoic attachment) in the chorion plate (Basyuk et al., 1999). *Gcm1* is essential for *Fzd5* upregulation in the chorion plate. After the chorioallantoic attachment, Wnt signaling is activated through *Fzd5*, which augments and maintains *Gcm1* expression (Lu et al., 2013). Thus the positive feedback mechanism between *Fzd5* and *Gcm1* is required for SynT-II cell differentiation and branch initiation of labyrinth villous (Anson-Cartwright et al., 2000; Lu et al., 2013). *Gcm1* only expresses in SynT-II layer in placenta, but not all SynT-II cells are positive for *Gcm1*. We showed in this study that induced SynT-II cells are *Gcm1* positive, indicating that the SynT-II cells are analogs of *Gcm1*-positive SynT-II cells *in vivo*. One of the best assays to confirm that *in vitro* differentiated cells are truly functional is to introduce such cells into early embryos and observe whether they integrate to the expected tissue. Several technical hurdles need to be overcome before such a procedure is used to confirm that SynT-II cells are capable of integrating into the SynT-II layer: the embryonic stage needs to be determined for SynT-II cell injection, prevention of miscarriage after reintroducing the SynT-II-injected embryos, etc. Alternatively, Wnt signaling may be activated genetically and labeled in a few Cdx2-positive cells using MADM-based mouse mosaic system at different stages in early embryos (Zong, 2014). Such manipulation may recapitulate the *in vitro* procedure of this report.

Previous observations showed that *Gcm1*-positive cells elongate and spread to form early labyrinth villous branches during initial morphogenesis (Cross et al., 2006). *In vivo*, the *Gcm1*-positive cells, as branching points, are not proliferating. Ectopically, expression of *Gcm1* in TSCs promotes rapid exit from the cell cycle *in vitro* (Hughes et al., 2004), suggesting that *Gcm1*-positive cells are post-mitotic, which was confirmed by phosphor histone H3 staining in placenta (Cross et al., 2006). Therefore,

Figure 5. c-MET/MAPK Signaling Is Required for SynT-II Cell Migration

(A) Invasive capability of undifferentiated TSCs and SynT-II cells in the transwell assays in the presence of indicated MEK1/2 or ROCK2 inhibitors.

(B) Invasive capability of SynT-II cells in the transwell assays in the presence of basic FGF and pan-FGFR or CXCR4 inhibitor.

(C) Invasive capability of SynT-II cells in the transwell assays in the presence of c-MET, bRAF, or MEK1/2 inhibitors.

(D) *c-Met* mRNA expression in TSCs and differentiated cells administrated with DMSO or CHIR. Data were summarized from three technical repeats, normalized to *Gapdh* expression, and represented as mean ± SEM.

(E) c-MET, MEK1/2 and phosphor-MEK1/2 expression measured by western blot assay in TSCs and CHIR-differentiated cells. β-Actin was used as loading control.

(F) Double immunofluorescent staining of c-MET and MCT4 in wild-type mouse placenta at E9.5, E10.5, and E12.5. Scale bar, 20 μm.

Data in (A), (B), and (C) were summarized from three experiments and represented as mean ± SEM. *$p < 0.05$; **$p < 0.01$; ***$p < 0.001$. ns, not significant.

See also Figures S5A and S5B.

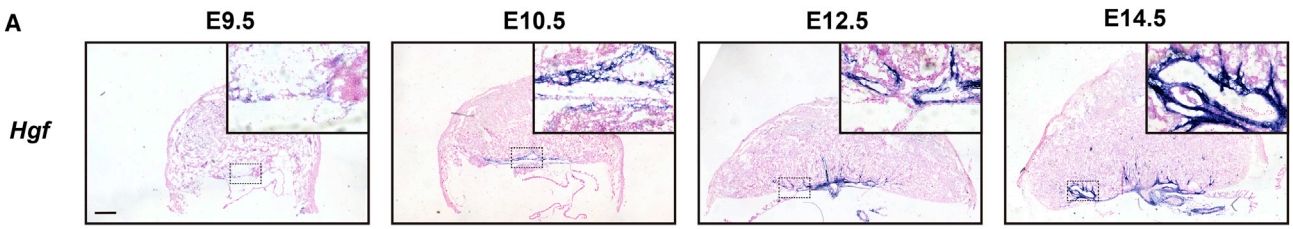

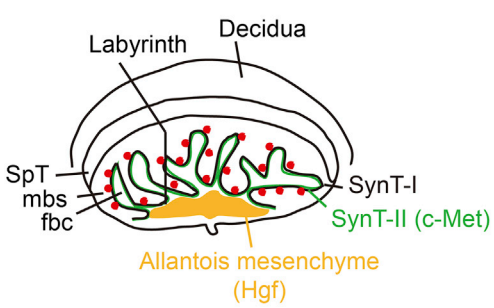

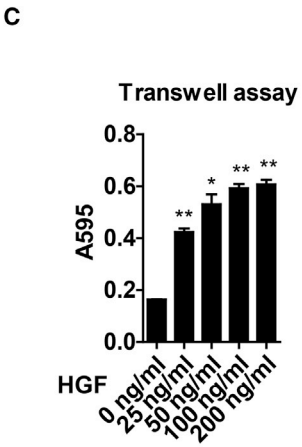

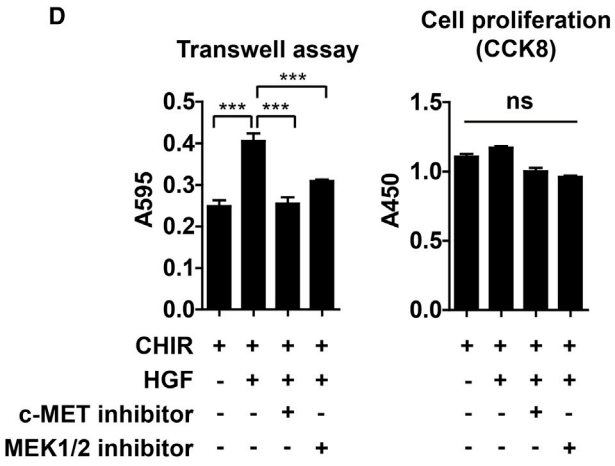

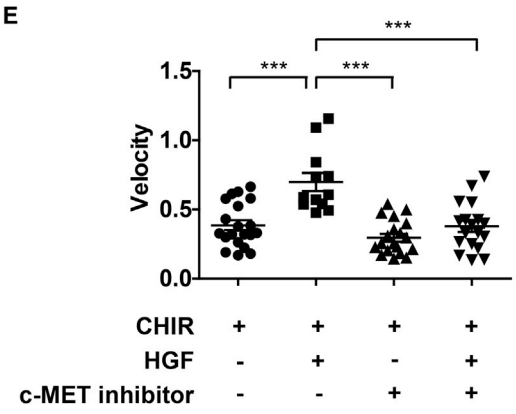

(legend on next page)

it was proposed that *Gcm1* cells might be pushed/squeezed as passengers by their surrounding proliferating cells. Our findings that SynT-II cells have migration and invasion capability suggest that SynT-II cells may have directional movement capability. We propose that *Gcm1*-positive cells at branching points are tip cells, which function similarly in branching morphogenesis of the vasculature system, leading their stalk cells to migrate and form labyrinth branches. Although it is unknown what mechanism underlies SynT-II cell directional migration, HGF/c-MET signaling is essential for SynT-II cell migration *in vitro*. In mouse placenta, HGF comes from the allantois mesoderm mesenchyme, while c-MET expresses in the SynT-II layer, suggesting that the ligand/receptor pair renders SynT-II cell migration capability *in vivo*. Although previous studies indicated that HGF could enhance proliferation of labyrinth trophoblast progenitor cells (Ueno et al., 2013) and increase outgrowth of trophoblasts from blastocysts (Patel et al., 2000), it is likely that the proliferation activity of HGF is not involved in migration of SynT-II cells. In contrast to *Gcm1*, which only shows discontinuous expression in the SynT-II layer, c-MET expresses in the whole layer. Whether *Gcm1*-positive tip cells are the only driving force *in vivo* remains to be investigated.

To control the appropriate size and shape, all branched tissues have a prominent common feature on regulating attraction and repulsion signaling pathways (Horowitz and Simons, 2009), which is usually achieved by balancing activities between chemo-attractants and chemo-repellents. HGF/c-MET signaling through intracellular MAPK regulates SynT-II cell migration, but it has no chemoattractant effect on SynT-II cells (data not shown). Besides Wnt and HGF, other signaling pathways, such as fibroblast growth factor, epidermal growth factor, and transforming growth factor β, have all been implicated in labyrinth morphogenesis (Watson and Cross, 2005). Hypoxia is also an important factor for labyrinth development (Burton, 2009; Pringle et al., 2010). Inactivation of hypoxia inducible factor 1α in maternal tissues significantly reduced *Gcm1* expression in labyrinth (Kenchegowda et al., 2017). In 0.5% O_2 culture condition, even with Fgf4 in the culture medium, TSCs were induced highly Gcm1 expression (Yang et al., 2016). Which molecules can function as a chemoattractant for SynT-II cells is obviously an interesting question. We propose that only the Gcm1-positive tip cells are able to react to the elusive chemoattractant. It is possible to use the *in vitro* SynT-II cells to screen endogenous chemoattractant.

EXPERIMENTAL PROCEDURES

See the Supplemental Experimental Procedures for additional details.

SynT-II Cells Differentiation

Mouse TSCs were cultured as described in the Supplemental Experimental Procedures. The mouse TSC line in this study was originally derived from E3.5 blastocysts by Dr. Janet Rossant's laboratory (The Hospital for Sick Children, University of Toronto).

To induce SynT-II cell differentiation, TSCs were cultured in TS medium in the absence of FGF4, heparin, and MEF-CM with addition of with 0.2 μM GSK3ixv (Millipore, 361558) or 3 μM CHIR 99021 (Stemgent, 04-0004) as indicated. The inhibitors were dissolved in DMSO. DMSO was used for vehicle control.

Cell Migration and Invasion Analysis

Cell motility was analyzed with wound-healing and transwell assays.

For the wound-healing assay, differentiated trophoblast cells induced by CHIR for 2 days were seeded onto 12-well plates coated with 5% RPMI-1640-diluted growth factor-reduced Matrigel (BD, 354230). After cells attached to the plate, the plate was scratched with a pipette tip to form wounds. Then pictures were taken at the indicated times.

Figure 6. HGF/c-MET Signaling Regulates SynT-II Cells Migration

(A) *Hgf* RNA expression in mouse placenta measured with *in-situ* hybridization at E9.5, E10.5, E12.5, and E14.5. Scale bar, 50 μm. The insets are the enlarged images in the rectangles.

(B) A diagram illustrating a mature mouse placenta and expression patterns of *c-Met* (green) and *Hgf* (yellow). SpT, spongiotrophoblast; mbs, maternal blood sinuses (red dots); fbc, fetal blood cell.

(C) Quantitative measurements of SynT-II cell invasiveness in transwell assays with HGF protein added in the lower chamber at indicated concentrations.

(D) Quantitative measurement of SynT-II cell invasiveness in transwell assays in the presence of 50 ng/μL HGF and/or c-MET inhibitor JNJ38877605 or MEK1/2 inhibitor PD0325901 (left panel). Right panel: proliferation of SynT-II cells measured with a CCK-8 kit, the cells were treated the same as in the left panel.

(E) Average velocities of SynT-II cells treated with HGF, and/or c-MET inhibitor JNJ38877605, were calculated by tracking single cell nuclei movement with ImageJ software.

Data in (C) and (D) were summarized from three experiments and represented as mean ± SEM. Data in (E) were summarized from two independent experiments. Cell numbers for each group (from left to right) are 20, 12, 19, and 18, respectively. *$p < 0.05$; **$p < 0.01$; ***$p < 0.001$. ns, not significant.

See also Figure S5C.

Boyden Chamber transwell assay (Corning, no. 3422) was used to monitor cell migration and invasion according to the manufacturer's instructions. Fifty microliters of cold 20% RPMI-1640-diluted growth factor-reduced Matrigel was coated on to the upper chamber of an 8-μm pore size transwell for 10 min in an incubator at 37°C with CO_2. The Matrigel was then aspirated out, then the transwells were air dried at room temperature. A total of 10^5 undifferentiated and 2-day differentiated trophoblast cells induced by indicated inhibitors were seeded into the upper chambers of Matrigel-coated transwells. The indicated inhibitors were added into the medium in both the upper and lower chambers. HGF (R&D, 294-HG, at the indicated concentrations) and basic FGF (PeproTech, 450-33, 100 ng/mL) were only added into the lower chamber as required. Two days later, cells were fixed with 4% paraformaldehyde for 5 min. After removing the cells on upper side of the transwell membrane using a cotton swab, cells left on the down side of the transwell were stained with 0.4% crystal violet for 15 min. After rinsing with water, the transwells were dried at room temperature. To quantify the cells that migrated through the transwell membranes, the crystal violet-stained cells were dissolved in 10% acetic acid, and then read at an absorbance of 595 nm (A_{595}) in a plate reader (Molecular Devices).

To analyze the expression profile of migrated cells through transwells, after removing the cells on the upper side of the membrane with a cotton swab, the cells left were lysed in Trizol solution, followed by RNA extraction and qPCR analysis. Cell proliferation was assayed with a CCK8 kit (Dojindo Laboratories, CK04). A total of 2×10^4 cells were seeded onto 96-well plates treated with the indicated inhibitors and/or HGF protein. The next day, after addition of 10 μL CCK8 into 100 μL cell medium for 2–4 hr, A_{450} absorption was read using a plate reader (Molecular Devices).

All the inhibitors used for the initial screening were kindly provided by National Compound Resource Center, China. The used inhibitor concentrations were listed in Table S1.

SUPPLEMENTAL INFORMATION

Supplemental Information includes Supplemental Experimental Procedures, five figures, two tables, and five movies and can be found with this article online at https://doi.org/10.1016/j.stemcr.2017.10.014.

AUTHOR CONTRIBUTIONS

D.Z. conceived the study, designed and performed experiments, analyzed data, and wrote the first draft of the manuscript. X.G. performed experiments and analyzed the data. L.M. and J.F. performed additional experiments. J.Z. conceived, supervised, supported the study, and finalized the manuscript.

ACKNOWLEDGMENTS

We thank Dr. Haibin Wang from Medical College of Xiamen University for providing *Gcm1*, *Tpbpa*, *Prl3d1*, and *Prl2c2* cDNA probes and Dr. Wei Wu from Tsinghua University for providing human wild-type and S37A mutant β-catenin plasmids. We thank the National Compound Resource Center (NCRC) for providing all the inhibitors used for the initial screening. This work was supported by grants from the National Natural Science Foundation of China (31590831, 31301195) and the Minister of Science and Technology China (2017YFA0504304).

Received: April 8, 2017
Revised: October 16, 2017
Accepted: October 17, 2017
Published: November 16, 2017

REFERENCES

Abell, A.N., Granger, D.A., Johnson, N.L., Vincent-Jordan, N., Dibble, C.F., and Johnson, G.L. (2009). Trophoblast stem cell maintenance by fibroblast growth factor 4 requires MEKK4 activation of Jun N-terminal kinase. Mol. Cell. Biol. *29*, 2748–2761.

Abell, A.N., Jordan, N.V., Huang, W., Prat, A., Midland, A.A., Johnson, N.L., Granger, D.A., Mieczkowski, P.A., Perou, C.M., Gomez, S.M., et al. (2011). MAP3K4/CBP-regulated H2B acetylation controls epithelial-mesenchymal transition in trophoblast stem cells. Cell Stem Cell *8*, 525–537.

Adamson, S.L., Lu, Y., Whiteley, K.J., Holmyard, D., Hemberger, M., Pfarrer, C., and Cross, J.C. (2002). Interactions between trophoblast cells and the maternal and fetal circulation in the mouse placenta. Dev. Biol. *250*, 358–373.

Anson-Cartwright, L., Dawson, K., Holmyard, D., Fisher, S.J., Lazzarini, R.A., and Cross, J.C. (2000). The glial cells missing-1 protein is essential for branching morphogenesis in the chorioallantoic placenta. Nat. Genet. *25*, 311–314.

Aoki, M., Mieda, M., Ikeda, T., Hamada, Y., Nakamura, H., and Okamoto, H. (2007). R-spondin3 is required for mouse placental development. Dev. Biol. *301*, 218–226.

Asanoma, K., Rumi, M.A., Kent, L.N., Chakraborty, D., Renaud, S.J., Wake, N., Lee, D.S., Kubota, K., and Soares, M.J. (2011). FGF4-dependent stem cells derived from rat blastocysts differentiate along the trophoblast lineage. Dev. Biol. *351*, 110–119.

Basyuk, E., Cross, J.C., Corbin, J., Nakayama, H., Hunter, P., Nait-Oumesmar, B., and Lazzarini, R.A. (1999). Murine Gcm1 gene is expressed in a subset of placental trophoblast cells. Dev. Dyn. *214*, 303–311.

Burton, G.J. (2009). Oxygen, the Janus gas; its effects on human placental development and function. J. Anat. *215*, 27–35.

Chen, C.P. (2014). Placental villous mesenchymal cells trigger trophoblast invasion. Cell Adh. Migr. *8*, 94–97.

Comijn, J., Berx, G., Vermassen, P., Verschueren, K., van Grunsven, L., Bruyneel, E., Mareel, M., Huylebroeck, D., and van Roy, F. (2001). The two-handed E box binding zinc finger protein SIP1 downregulates E-cadherin and induces invasion. Mol. Cell *7*, 1267–1278.

Cross, J.C., Nakano, H., Natale, D.R., Simmons, D.G., and Watson, E.D. (2006). Branching morphogenesis during development of placental villi. Differentiation *74*, 393–401.

Dokras, A., Gardner, L.M., Seftor, E.A., and Hendrix, M.J. (2001). Regulation of human cytotrophoblast morphogenesis by hepatocyte growth factor/scatter factor. Biol. Reprod. *65*, 1278–1288.

Hatano, N., Mori, Y., Oh-hora, M., Kosugi, A., Fujikawa, T., Nakai, N., Niwa, H., Miyazaki, J., Hamaoka, T., and Ogata, M. (2003).

Essential role for ERK2 mitogen-activated protein kinase in placental development. Genes Cells *8*, 847–856.

Hayakawa, K., Himeno, E., Tanaka, S., and Kunath, T. (2015). Isolation and manipulation of mouse trophoblast stem cells. Curr. Protoc. Stem Cell Biol. *32*, 1E.4.1–1E.4.32.

Hemberger, M., Hughes, M., and Cross, J.C. (2004). Trophoblast stem cells differentiate in vitro into invasive trophoblast giant cells. Dev. Biol. *271*, 362–371.

Hidalgo-Carcedo, C., Hooper, S., Chaudhry, S.I., Williamson, P., Harrington, K., Leitinger, B., and Sahai, E. (2011). Collective cell migration requires suppression of actomyosin at cell-cell contacts mediated by DDR1 and the cell polarity regulators Par3 and Par6. Nat. Cell Biol. *13*, 49–58.

Horowitz, A., and Simons, M. (2009). Branching morphogenesis. Circ. Res. *104*, e21.

Hughes, M., Dobric, N., Scott, I.C., Su, L., Starovic, M., St-Pierre, B., Egan, S.E., Kingdom, J.C., and Cross, J.C. (2004). The Hand1, Stra13 and Gcm1 transcription factors override FGF signaling to promote terminal differentiation of trophoblast stem cells. Dev. Biol. *271*, 26–37.

Huppertz, B., and Gauster, M. (2011). Trophoblast fusion. Adv. Exp. Med. Biol. *713*, 81–95.

Imamura, R., and Matsumoto, K. (2017). Hepatocyte growth factor in physiology and infectious diseases. Cytokine *98*, 97–106.

Ishikawa, T., Tamai, Y., Zorn, A.M., Yoshida, H., Seldin, M.F., Nishikawa, S., and Taketo, M.M. (2001). Mouse Wnt receptor gene Fzd5 is essential for yolk sac and placental angiogenesis. Development *128*, 25–33.

Kenchegowda, D., Natale, B., Lemus, M.A., Natale, D.R., and Fisher, S.A. (2017). Inactivation of maternal Hif-1alpha at mid-pregnancy causes placental defects and deficits in oxygen delivery to the fetal organs under hypoxic stress. Dev. Biol. *422*, 171–185.

Lu, J., Zhang, S., Nakano, H., Simmons, D.G., Wang, S., Kong, S., Wang, Q., Shen, L., Tu, Z., Wang, W., et al. (2013). A positive feedback loop involving Gcm1 and Fzd5 directs chorionic branching morphogenesis in the placenta. PLoS Biol. *11*, e1001536.

Ma, H.T., and Poon, R.Y. (2017). Synchronization of HeLa cells. Methods Mol. Biol. *1524*, 189–201.

Maltepe, E., Bakardjiev, A.I., and Fisher, S.J. (2010). The placenta: transcriptional, epigenetic, and physiological integration during development. J. Clin. Invest. *120*, 1016–1025.

Matsuura, K., Jigami, T., Taniue, K., Morishita, Y., Adachi, S., Senda, T., Nonaka, A., Aburatani, H., Nakamura, T., and Akiyama, T. (2011). Identification of a link between Wnt/beta-catenin signalling and the cell fusion pathway. Nat. Commun. *2*, 548.

Mikkola, H.K., Gekas, C., Orkin, S.H., and Dieterlen-Lievre, F. (2005). Placenta as a site for hematopoietic stem cell development. Exp. Hematol. *33*, 1048–1054.

Moffett, A., and Loke, C. (2006). Immunology of placentation in eutherian mammals. Nat. Rev. Immunol. *6*, 584–594.

Monkley, S.J., Delaney, S.J., Pennisi, D.J., Christiansen, J.H., and Wainwright, B.J. (1996). Targeted disruption of the Wnt2 gene results in placentation defects. Development *122*, 3343–3353.

Nagai, A., Takebe, K., Nio-Kobayashi, J., Takahashi-Iwanaga, H., and Iwanaga, T. (2010). Cellular expression of the monocarboxylate transporter (MCT) family in the placenta of mice. Placenta *31*, 126–133.

Nakamura, T., Sakai, K., Nakamura, T., and Matsumoto, K. (2011). Hepatocyte growth factor twenty years on: much more than a growth factor. J. Gastroenterol. Hepatol. *1* (26 Suppl), 188–202.

Nasu, K., Zhou, Y., McMaster, M.T., and Fisher, S.J. (2000). Upregulation of human cytotrophoblast invasion by hepatocyte growth factor. J. Reprod. Fertil. Suppl. *55*, 73–80.

O'Brien, L.E., Tang, K., Kats, E.S., Schutz-Geschwender, A., Lipschutz, J.H., and Mostov, K.E. (2004). ERK and MMPs sequentially regulate distinct stages of epithelial tubule development. Dev. Cell *7*, 21–32.

Parr, B.A., Cornish, V.A., Cybulsky, M.I., and McMahon, A.P. (2001). Wnt7b regulates placental development in mice. Dev. Biol. *237*, 324–332.

Patel, Y., Kim, H., and Rappolee, D.A. (2000). A role for hepatocyte growth factor during early postimplantation growth of the placental lineage in mice. Biol. Reprod. *62*, 904–912.

Pringle, K.G., Kind, K.L., Sferruzzi-Perri, A.N., Thompson, J.G., and Roberts, C.T. (2010). Beyond oxygen: complex regulation and activity of hypoxia inducible factors in pregnancy. Hum. Reprod. Update *16*, 415–431.

Quinn, J., Kunath, T., and Rossant, J. (2006). Mouse trophoblast stem cells. Methods Mol. Med. *121*, 125–148.

Rai, A., and Cross, J.C. (2015). Three-dimensional cultures of trophoblast stem cells autonomously develop vascular-like spaces lined by trophoblast giant cells. Dev. Biol. *398*, 110–119.

Ridley, A.J. (2015). Rho GTPase signalling in cell migration. Curr. Opin. Cell Biol. *36*, 103–112.

Robin, C., Bollerot, K., Mendes, S., Haak, E., Crisan, M., Cerisoli, F., Lauw, I., Kaimakis, P., Jorna, R., Vermeulen, M., et al. (2009). Human placenta is a potent hematopoietic niche containing hematopoietic stem and progenitor cells throughout development. Cell Stem Cell *5*, 385–395.

Rossant, J., and Cross, J.C. (2001). Placental development: lessons from mouse mutants. Nat. Rev. Genet. *2*, 538–548.

Simmons, D.G., Fortier, A.L., and Cross, J.C. (2007). Diverse subtypes and developmental origins of trophoblast giant cells in the mouse placenta. Dev. Biol. *304*, 567–578.

Simmons, D.G., Natale, D.R., Begay, V., Hughes, M., Leutz, A., and Cross, J.C. (2008a). Early patterning of the chorion leads to the trilaminar trophoblast cell structure in the placental labyrinth. Development *135*, 2083–2091.

Simmons, D.G., Rawn, S., Davies, A., Hughes, M., and Cross, J.C. (2008b). Spatial and temporal expression of the 23 murine prolactin/placental lactogen-related genes is not associated with their position in the locus. BMC Genomics *9*, 352.

Somerset, D.A., Li, X.F., Afford, S., Strain, A.J., Ahmed, A., Sangha, R.K., Whittle, M.J., and Kilby, M.D. (1998). Ontogeny of hepatocyte growth factor (HGF) and its receptor (c-met) in human placenta: reduced HGF expression in intrauterine growth restriction. Am. J. Pathol. *153*, 1139–1147.

Sonderegger, S., Pollheimer, J., and Knofler, M. (2010). Wnt signalling in implantation, decidualisation and placental differentiation – review. Placenta *31*, 839–847.

Tanaka, S., Kunath, T., Hadjantonakis, A.K., Nagy, A., and Rossant, J. (1998). Promotion of trophoblast stem cell proliferation by FGF4. Science *282*, 2072–2075.

Tremblay, G.B., Kunath, T., Bergeron, D., Lapointe, L., Champigny, C., Bader, J.A., Rossant, J., and Giguere, V. (2001). Diethylstilbestrol regulates trophoblast stem cell differentiation as a ligand of orphan nuclear receptor ERR beta. Genes Dev. *15*, 833–838.

Uehara, Y., Minowa, O., Mori, C., Shiota, K., Kuno, J., Noda, T., and Kitamura, N. (1995). Placental defect and embryonic lethality in mice lacking hepatocyte growth factor/scatter factor. Nature *373*, 702–705.

Ueno, M., Lee, L.K., Chhabra, A., Kim, Y.J., Sasidharan, R., Van Handel, B., Wang, Y., Kamata, M., Kamran, P., Sereti, K.I., et al. (2013). c-Met-dependent multipotent labyrinth trophoblast progenitors establish placental exchange interface. Dev. Cell *27*, 373–386.

Unek, G., Ozmen, A., Isenlik, B.S., and Korgun, E.T. (2017). The proliferation mechanism of normal and pathological human placentas. Histol. Histopathol. *32*, 339–349.

Watson, E.D., and Cross, J.C. (2005). Development of structures and transport functions in the mouse placenta. Physiology (Bethesda) *20*, 180–193.

Yan, J., Tanaka, S., Oda, M., Makino, T., Ohgane, J., and Shiota, K. (2001). Retinoic acid promotes differentiation of trophoblast stem cells to a giant cell fate. Dev. Biol. *235*, 422–432.

Yang, J., and Weinberg, R.A. (2008). Epithelial-mesenchymal transition: at the crossroads of development and tumor metastasis. Dev. Cell *14*, 818–829.

Yang, Y., Arenas-Hernandez, M., Gomez-Lopez, N., Dai, J., Parker, G.C., Puscheck, E.E., and Rappolee, D.A. (2016). Hypoxic stress forces irreversible differentiation of a majority of mouse trophoblast stem cells despite FGF4. Biol. Reprod. *95*, 110.

Zong, H. (2014). Generation and applications of MADM-based mouse genetic mosaic system. Methods Mol. Biol. *1194*, 187–201.